Subpicosecond plasmon response: Buildup of screening

K. El Sayed, S. Schuster, and H. Haug
Institut für Theoretische Physik, Universität Frankfurt, Robert-Mayer-Strasse 8, D-60054 Frankfurt a.M., Germany

F. Herzel and K. Henneberger
Fachbereich Physik, Abteilung Theoretische Physik, Universität Rostock, Universitätsplatz 3, D-18051 Rostock, Germany

(Received 26 October 1993)

The screened Coulomb Keldysh propagator is evaluated in the time-domain for ultra-short-pulse laser excitation of a semiconductor using the nonequilibrium Green-function technique. The buildup of screening in the time interval during and shortly after the pulse excitation is treated. A time-dependent plasmon-pole approximation is derived and shown to give an excellent description of the dynamics of screening after a resonant femtosecond pulse.

I. INTRODUCTION

In the past few years four-wave-mixing and time-resolved luminescence experiments have been performed on bulk and quantum well semiconductors. The crystals have been excited by laser pulses with durations of several 10 fs. The polarization decay and carrier relaxation have been measured.[1–5] In these experiments very short polarization decay times have been found which were always close to the time resolution. In Refs. 6–8 the short scattering times have been tentatively explained as a new plasmon resonance effect which is only present if the carrier distribution is far from equilibrium. The corresponding analysis is based on the Lindhard formula for the dynamically screened Coulomb potential.[9] This approach is, strictly speaking, only justified if the carrier distributions are slowly changing in time. In this paper we will relax this condition by using the Keldysh nonequilibrium Green function technique. We analyze the evolution of the screened Coulomb potential, i.e., the density-density correlation function, in the time domain. The understanding of this correlation function is essential for the description of the buildup of screening in an electron-hole plasma on ultra-short-time scales and for the Coulomb quantum kinetics.[10–14] Quantum kinetics generalizes the Markovian Boltzmann transport and scattering theory in the initial time interval, in which the energy uncertainty is comparable to the kinetic energy of the carriers. In this regime non-Markovian memory effects have to be taken into account.

The paper is organized as follows: In Sec. II a closed set of equations for the Keldysh Green functions of the carriers and of the screened Coulomb potential is given in the random phase approximation (RPA). In Sec. III the free generalized Kadanoff-Baym approximation (FGKB) is introduced. This approximation allows us to express the RPA equations in terms of the one-particle reduced density matrix, i.e., the carrier distributions and the optical polarization. In Sec. IV a two-time-dependent plasmon pole approximation for the spectral screened Coulomb potential Green function, i.e., the retarded and the advanced Green function, is developed. During and shortly after an excitation with an ultrashort laser pulse it is possible to solve the coupled equation of the reduced density matrix and the screened Coulomb potential iteratively. The first-order equations of the reduced density matrix are the Hartree-Fock semiconductor Bloch equations which are given in Sec. V. In Sec. VI the numerical solution of the semiconductor Bloch equations are used to calculate the density-density correlation function. A partial Fourier transform from the two-time-dependent potential is introduced. This quantity which describes the buildup of screening on the femtosecond time scale is compared with the plasmon pole approximation of Sec. IV. An excellent agreement is found.

In the forthcoming second section we will investigate the kinetic Green functions V^{+-} and V^{-+}. These particlelike elements describe the plasmon distribution. We will follow the evolution of the plasmon distribution from the initial creation of nonequilibrium plasmons to the final equilibrium Bose distribution.

II. CLOSED SET OF DYSON EQUATIONS

The Keldysh nonequilibrium Green function matrix is defined as

$$G^{z_1 z_2}_{b_1 b_2 k}(t_1,t_2) = \frac{1}{i}\begin{pmatrix} \langle T\psi_{b_1 k}(t_1)\psi^\dagger_{b_2 k}(t_2)\rangle & \langle \psi^\dagger_{b_2 k}(t_2)\psi_{b_1 k}(t_1)\rangle \\ \langle \psi_{b_1 k}(t_1)\psi^\dagger_{b_2 k}(t_2)\rangle & \langle \tilde{T}\psi_{b_1 k}(t_1)\psi^\dagger_{b_2 k}(t_2)\rangle \end{pmatrix}. \tag{2.1}$$

0163-1829/94/49(11)/7337(8)/$06.00

©1994 The American Physical Society

Here $z = \pm 1$ is the Keldysh contour index, T ($\tilde{T}$) is the time-ordering (anti-time-ordering) operator, $b = (c, v)$ is the band index for the conduction and valence band of a two-band model, k the carrier momentum. The electron field operators ψ are in the Heisenberg picture. The vector notation is suppressed; $\hbar = 1$ is used.

In the framework of the nonequilibrium Keldysh technique the Dyson equation for the particle propagator reads[9,15,16]

$$G^{z_1 z_2}_{b_1 b_2 k}(t_1, t_2) = \delta_{b_1 b_2} G^{0 z_1 z_2}_{b_1 k}(t_1, t_2) + \sum_{z_3 z_4 b_3} \int dt_3 dt_4 G^{0 z_1 z_3}_{b_1 k}(t_1, t_3) \Sigma^{z_3 z_4}_{b_1 b_3 k}(t_3, t_4) G^{z_4 z_2}_{b_3 b_2 k}(t_4, t_2). \tag{2.2}$$

We use the notation of Ref. 9. Within the random phase approximation (RPA) the self-energy is given by

$$\Sigma^{z_1 z_2}_{b_1 b_2 k}(t_1, t_2) = i z_2 \sum_k V^{z_1 z_2}_q(t_1, t_2) G^{z_1 z_2}_{b_1 b_2 k-q}(t_1, t_2) - \delta(t_1 - t_2) \delta_{z_1 z_2} d_k E(t_1)(1 - \delta_{b_1 b_2}). \tag{2.3}$$

The last term of Eq. (2.3) describes the interaction with an external classical laser field $E(t)$. In the following the interband optical matrix element d_k is assumed to be constant. V is the two-time Keldysh potential propagator of the screened Coulomb potential. To be precise, in equilibrium the Fourier transform with respect to the relative time $t = t_1 - t_2$ of the retarded potential propagator gives the well-known dynamically screened Coulomb potential. The Dyson equation for the Keldysh potential matrix is (see also Ref. 17)

$$V^{z_1 z_2}_q(t_1, t_2) = V_q \delta(t_1 - t_2) \delta_{z_1 z_2} + \sum_{z_3} \int dt_3 V_q L^{z_1 z_3}_q(t_1, t_3) V^{z_3 z_2}_q(t_3, t_2) \tag{2.4}$$

with

$$V_q = \frac{a_0^3 E_0}{\Omega} \frac{8\pi}{(q a_0)^2}.$$

V is the bare Coulomb potential, here given in units of the exciton Bohr radius a_0 and the exciton Ryberg E_0. Ω is the normalization volume. The polarization bubble L in the RPA is given by

$$L^{z_1 z_2}_q(t_1, t_2) = -i z_1 \sum_{b_1 b_2 k} G^{z_1 z_2}_{b_1 b_2 k+q}(t_1, t_2) G^{z_2 z_1}_{b_2 b_1 k}(t_2, t_1). \tag{2.5}$$

Equations (2.2)–(2.5) form a closed set of equations. Unfortunately, this set is too complex to be solved without further approximations.

III. SIMPLIFYING APPROXIMATIONS

In most circumstances the knowledge of the full two-time Keldysh matrix is not required; often it is sufficient to know only the one-particle reduced density matrix

$$\rho_{b_1 b_2 k}(t) = \begin{pmatrix} n_{ck}(t) & P^*_k(t) \\ P_k(t) & n_{vk}(t) \end{pmatrix} = i G^{+-}_{b_1 b_2 k}(t, t), \tag{3.1}$$

i.e., the equal-time limit of the Keldysh matrix G^{+-}. n_{bk} is the carrier distribution and P_k is the polarization. Unfortunately, the time-diagonal elements of the Keldysh matrix have no closed description on the basis of Eqs. (2.2)–(2.5). Kadanoff and Baym (KB) (Ref. 18) used the equilibrium relation between the two-time Green function and the density matrix. Lipavský and co-workers[13] improved the KB ansatz by including the causality properly. Their generalization of the KB for two bands reads (GKB)

$$G^{+-}_{b_1 b_2 k}(t_1, t_2) = i \sum_{b_3} \Big[G^r_{b_1 b_3 k}(t_1, t_2) G^{+-}_{b_3 b_2 k}(t_2, t_2) - G^{+-}_{b_1 b_3 k}(t_1, t_1) G^a_{b_3 b_2 k}(t_1, t_2) \Big]. \tag{3.2}$$

The ansatz for G^{-+} looks alike. The GKB ansatz closes the set of equations for the reduced density matrices. The two-time retarded and advanced Green functions are linear combinations of the elements of the Keldysh matrix, e.g.,

$$G^r = G^{++} + G^{+-} = G^{--} + G^{-+},$$

$$G^a_{b_1 b_2 k}(t_1, t_2) = \left[G^r_{b_2 b_1 k}(t_2, t_1) \right]^*. \tag{3.3}$$

The potential propagator obeys a similar equation. The spectral propagators G^r and G^a will at this point be approximated by the free-particle propagators with renormalized quasi-particle energies in the form of a constant shift and a damping γ. Because in the final results only energy differences will appear, we drop the constant en-

ergy shift and get

$$G_b^{0r}(t_1,t_2)=\frac{1}{i}\Theta(t_1-t_2)e^{-i(\epsilon_{bk}-i\gamma)(t_1-t_2)}. \tag{3.4}$$

This approximation neglects the off-diagonal elements of the spectral propagators. These off-diagonal propagators contribute already in first order of the exciting laser field.[19] In Ref. 20 it has been shown for an interaction with longitudinal-optical (LO) phonons that these elements are needed in steady state for a consistent description of the phonon-assisted absorption sidebands. However, for short pulse excitation these band-mixing effects are mainly important during the laser pulse. The relevant time scale for the buildup of screening will be shown to be a characteristic inverse plasma frequency. Therefore, the approximation (3.4) is justified if this inverse plasma frequency exceeds the pulse duration. A consistent description of the spectral *and* kinetic equations is delicate and will certainly need further consideration.

This modified GKB ansatz, which may be called free GKB (FGKB) ansatz, reads

$$G^{+-}_{b_1b_2k}(t_1,t_2)=i\Big[G^{0r}_{b_1k}(t_1,t_2)G^{+-}_{b_1b_2k}(t_2,t_2) -G^{+-}_{b_1b_2k}(t_1,t_1)G^{0a}_{b_2k}(t_1,t_2)\Big]. \tag{3.5}$$

It is consistent with, e.g., the Boltzmann equation or the Lindhard formula. Within the FGKB ansatz the equations of the density matrix are already closed. It is convenient to formulate these equations as differential equations, which are derived by standard techniques (i.e., multiplying both sides of the Dyson equation with the differential operator of the inverse free-particle Green function G^{0-1} once from the left and once from the right, and take the difference of both equations).[15,18]

The Dyson equation for the retarded potential propagators V^r reads

$$V_q^r(t_1,t_2)=\delta(t_1-t_2)V_q + \int_{t_2}^{t_1}dt_3V_qL_q^r(t_1,t_3)V_q^r(t_3,t_2). \tag{3.6}$$

Using Eq. (3.5), the retarded polarization bubble becomes

$$\begin{aligned}L_q^r(t_1,t_2)&=\Theta(t_1-t_2)\left[L_q^{+-}(t_1,t_2)+L_q^{-+}(t_1,t_2)\right]\\ &=-i\Theta(t_1-t_2)\sum_{bk}e^{i(\epsilon_{bk}-\epsilon_{bk+q}+i2\gamma)(t_1-t_2)}\\ &\quad\times\left[n_{bk}(t_2)-n_{bk+q}(t_2)\right].\end{aligned} \tag{3.7}$$

In FGKB the interband polarization P_k does not contribute to L_q^r, because we have neglected band-mixing effects [see Eq. (3.4)]. If the distribution function is isotropic in momentum space, L^r is real. These properties are passed from L_q^r to V_q^r. Corresponding to Eq. (3.3), it is sufficient to know the retarded potential propagator V_q^r. The component V^{+-} can be evaluated using

$$V_q^{+-}(t_1,t_2)=\int_{-\infty}^{t_1}dt_3\int_{-\infty}^{t_2}dt_4V_q^r(t_1,t_3) \times L_q^{+-}(t_3,t_4)V_q^a(t_4,t_2). \tag{3.8}$$

A similar equation for V^{-+} holds.[10,17]

IV. TIME-DEPENDENT PLASMON-POLE APPROXIMATION

The long-wavelength limit of the polarization function leads to a generalization of the plasma frequency.

$$\lim_{q\to0}V_qL_q^r(t_1,t_2) =-(t_1-t_2)\Theta(t_1-t_2)e^{-2\gamma(t_1-t_2)}\omega_{\rm pl}^2(t_2), \tag{4.1}$$

with

$$\omega_{\rm pl}^2(t)=E_0^2 16\pi a_0^3\sum_b\frac{\mu}{m_b}n_b(t),$$
$$n_b(t)=2\sum_k n_{bk}(t), \tag{4.2}$$

where m_b are the band masses and μ the reduced electron-hole mass. This result defines the plasma frequency $\omega_{\rm pl}(t)$ in terms of the total density $n_b(t)$ of any nonequilibrium distribution. The factor of 2 in the definition of the total density accounts for the spin degeneracy.

Next we rewrite the Dyson equation (3.6) for the retarded screened Coulomb potential by introducing the density-density correlation function $S_q(t_1,t_2)$ in the form

$$V_q^r(t_1,t_2)=V_q\left[\delta(t_1-t_2)+S_q(t_1,t_2)e^{-2\gamma(t_1-t_2)}\right]. \tag{4.3}$$

The trivial damping constants γ from the damped free-particle Green functions are taken explicitly into account. For the screening described by the density-density correlation function only the Landau damping contributes. A comparison of Eqs. (3.6) and (4.3) yields

$$S_q(t_1,t_2)=V_qL_q^r(t_1,t_2) + \int_{t_2}^{t_1}dt_3V_qL_q^r(t_1,t_3)S_q(t_3,t_2). \tag{4.4}$$

The polarization $L_q^r(t_1,t_3)$ has to be evaluated with $\gamma=0$. For the long-wavelength limit of (4.4) we find with (4.1) the differential equation of a parametric oscillator

$$\frac{d^2}{dt_1^2}S_{q=0}(t_1,t_2)=-\omega_{\rm pl}^2(t_1)S_{q=0}(t_1,t_2). \tag{4.5}$$

This equation shows that the long-wavelength limit density-density correlation function oscillates with the actual plasma frequency which may change parametrically with time t_1 as the plasma density $n(t_1)$ changes. Furthermore, one finds the following initial conditions:

$$S_{q=0}(t_2,t_2)=0$$

and

$$\frac{d}{dt_1}S_{q=0}(t_1,t_2)|_{t_1\to t_2} = -\omega_{\rm pl}^2(t_2), \tag{4.6}$$

where we used $\lim_{q\to 0}\Theta(t_1-t_2)=1$.

Equations (4.6) are the nonequilibrium generalization of the well-known sum rule[21]

$$\int_0^\infty d\omega\omega {\rm Im}\left[\epsilon_q^{-1}(\omega)\right] = -\frac{\pi}{2}\omega_{\rm pl}^2. \tag{4.7}$$

We solve Eq. (4.5) with the ansatz

$$S_{q=0}(t_1,t_2) = \tilde{S}(t_1,t_2)\exp\left(-i\int_{t_2}^{t_1} d\tau\omega_{\rm pl}(\tau)\right). \tag{4.8}$$

$\tilde{S}(t_1,t_2)=s(t_1)$ obeys the following equation of motion in t_1:

$$\ddot{s} - i\dot{\omega}_{\rm pl}s - 2i\omega_{\rm pl}\dot{s} = 0. \tag{4.9}$$

We assume that the parametric changes of $\omega_{\rm pl}(t_1)$ are sufficiently small in an oscillation period, so that the second-order derivative of s can be neglected. The remaining equation can be solved by separation of variables. We find

$$\frac{ds}{s} = -\frac{1}{2}\frac{d\omega_{\rm pl}}{\omega_{\rm pl}}, \tag{4.10}$$

with the solution

$$s(t_1) = \tilde{S}(t_1,t_2) = S_0\omega_{\rm pl}^{-1/2}(t_1)\omega_{\rm pl}^{1/2}(t_2). \tag{4.11}$$

The first initial condition (4.6) yields

$$S_{q=0}(t_1,t_2) = -iS_0\omega_{\rm pl}^{-1/2}(t_1)\omega_{\rm pl}^{1/2}(t_2) \times\sin\left(\int_{t_2}^{t_1} dt_3\omega_{\rm pl}(t_3)\right). \tag{4.12}$$

The second initial condition (4.6) at $t_1=t_2$ determines $S_0=-i\omega_{\rm pl}(t_2)$.

The final long-wavelength limit of the time-dependent density-density correlation is in the plasmon-pole approximation,

$$S_{q=0}(t_1,t_2) = -\Theta(t_1-t_2)\omega_{\rm pl}^{3/2}(t_2)\omega_{\rm pl}^{-1/2}(t_1) \times\sin\left(\int_{t_2}^{t_1} dt_3\omega_{\rm pl}(t_3)\right). \tag{4.13}$$

Before we can insert $S_q(t_1,t_2)$ into Eq. (4.3) we have to extend it to finite q values. This can be done by comparing the Fourier transform of the equilibrium density-density correlation $S_q^0(\omega)$ in the plasmon pole approximation[22] with respect to the relative time coordinate t_1-t_2 with (4.13). In equilibrium the time-dependent plasmon-pole approximation is[10]

$$S_q^0(t_1-t_2) = \int_{-\infty}^{+\infty}\frac{d\omega}{2\pi}e^{-i\omega(t_1-t_2)}\frac{\omega_{\rm pl}^2}{(\omega+i\delta)^2-\omega_q^2} = -\Theta(t_1-t_2)\frac{\omega_{\rm pl}^2}{\omega_q}\sin\left[\omega_q(t_1-t_2)\right], \tag{4.14}$$

with the dispersion of the effective plasmon pole

$$\omega_q^2 = \omega_{\rm pl}^2\left(1+\frac{q^2}{\kappa^2}\right) + Cq^4. \tag{4.15}$$

The inverse screening length κ can be expressed in a form which can be used also for nonequilibrium distributions:

$$\kappa^2 = \frac{8}{\pi a_0}\sum_b\frac{m_b}{\mu}\int_0^\infty dk\, n_{bk}, \tag{4.16}$$

assuming that the (nonequilibrium) distribution is isotropic, i.e., depends only $|k|$. C is a numerical constant. A detailed discussion of the plasmon dispersion in nonequilibrium is given in Ref. 7. The comparison between (4.13) and (4.14) shows that at finite q values one has to use the following nonequilibrium density-density correlation:

$$S_q(t_1,t_2) = -\Theta(t_1-t_2)\frac{\omega_{\rm pl}^2(t_2)}{\omega_q^{1/2}(t_1)\omega_q^{1/2}(t_2)} \times\sin\left(\int_{t_2}^{t_1} dt_3\omega_q(t_3)\right). \tag{4.17}$$

Naturally the time-dependent frequencies $\omega_{pl}(t)$ and $\omega_q(t)$ have to be calculated from time-dependent $n_{bk}(t)$. With this result the nonequilibrium damped plasmon pole approximation for the retarded screened Coulomb potential is obtained with (4.3) as

$$V_q^r(t_1,t_2) = V_q\left[\delta(t_1-t_2) - \Theta(t_1-t_2)\frac{\omega_{\rm pl}^2(t_2)}{\omega_q^{1/2}(t_1)\omega_q^{1/2}(t_2)}\sin\left(\int_{t_2}^{t_1} dt_3\omega_q(t_3)\right)e^{-\gamma(t_1-t_2)}\right]. \tag{4.18}$$

Equation (4.17) shows that the initial amplitude of the density correlation function depends on the $\omega_{\rm pl}(t_2)$, especially if $\omega_{\rm pl}(t_2)=0$, i.e., vacuum state at t_2; S_q will stay zero for all later times t_1. We conclude further that any change in the frequency ω_q will cause a change in the amplitude, which is well known for parametric oscillators. In Eq. (4.17) the Landau damping is not included. It can be described by an extra factor

$$\exp\left(-\int_{t_2}^{t_1} dt_3\gamma_q(t_3)\right). \tag{4.19}$$

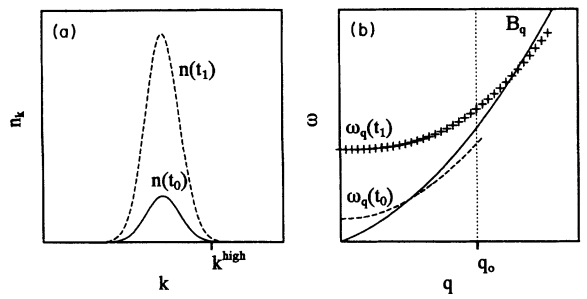

FIG. 1. (a) Two snapshots of a time-dependent carrier distribution n_k versus momentum k. (b) The corresponding plasmon dispersions ω_q versus momentum qa_0. The solid line shows the boundary of the pair continuum, beyond which the plasmon is strongly damped.

Numerical studies with test distributions have shown that this damping can have a rather complex time dependence, which can be illustrated by a simple Gedanken experiment (see Fig. 1): Assume that the distribution is initially at t_0 narrow in momentum space, e.g., a narrow Gaussian distribution. Between t_0 and t_1 its amplitude is increasing. The boundary of the pair continuum is approximately given by

$$B_q = \frac{2k^{\text{high}}q + q^2}{m_c}, \tag{4.20}$$

where k^{high} is a characteristic momentum of the high-energy tail of the carrier distribution. Obviously this boundary will not change in the interval $[t_0, t_1]$, while the plasma frequency is increasing with the square root of the carrier density. For a momentum q_0 the dispersion ω_q may be initially inside the continuum and strongly damped. While the mode shifts to higher energies it may leave the continuum and will oscillate without Landau damping until the distribution gets broadened due to scattering. Then the boundaries of the continuum are smeared out. In general, the Landau damping $\gamma_q(t)$ cannot be calculated easily and will change with time. But we expect that for many situations also a simple modeling of the Landau damping will give reasonable results, as is the case in equilibrium.[22]

V. SHORT TIME DYNAMICS

$V_q^r(t_1, t_2)$ is an oscillating function of t_1 for fixed t_2. The frequency of the oscillation is given by the plasmon dispersion ω_q at time t_1. For moderate densities in GaAs, e.g., the plasma frequency is of the order of 100 fs (for $n = 3.6 \times 10^{17}$ cm^{-3}, $\omega_{\text{pl}} \simeq 30$ meV, corresponding to a period of 140 fs). For optical excitations with ultrashort laser pulses of several 10 fs pulse width, it is possible to use an iterative scheme in order to solve the problem. In the first step the kinetic equations, i.e., the differential equations for the G^{+-}, are solved taking only the bare Coulomb potential into account. The resulting well-known semiconductor Bloch equations[9,23] for the polarization and the carrier distributions are

$$\begin{aligned} i\frac{d}{dt}P_k(t) &= [e_{ck}(t) - e_{vk}(t) - i2\gamma]\,P_k(t) \\ &\quad - [n_{vk}(t) - n_{ck}(t)]\,\Omega_k^R(t), \\ \frac{d}{dt}n_{ck}(t) &= -2\,\text{Im}\left[\Omega_k^R(t)P_k^*(t)\right], \\ n_{vk}(t) &= 1 - n_{ck}(t). \end{aligned} \tag{5.1}$$

The laser field causes direct transitions from the valence to the conduction band. This correlation of the electron and hole distribution will be destroyed by incoherent scattering, which leads to an intraband relaxation. In the first step of the iterative scheme scattering is not considered at all. e_{bk} are the Hartree-Fock renormalized single-particle energies and Ω_k^R the renormalized Rabi frequency.

$$\begin{aligned} e_{ck}(t) &= \epsilon_{ck} - \sum_q V_q n_{ck-q}(t), \\ e_{vk}(t) &= \epsilon_{vk} - \sum_q V_q[1 - n_{vk-q}(t)], \\ \Omega_k^R &= dE(t) + \sum_q V_q P_{k-q}(t). \end{aligned} \tag{5.2}$$

Again we introduced a phenomenological polarization damping in agreement with Eq. (3.4). Within the rotating wave approximation $E(t)$ denotes only the pulse envelope function, while the band gap E_g is shifted by the central frequency of the pulse ω_0. The unrenormalized single-particle energies are

$$\begin{aligned} \epsilon_{ck} &= \frac{k^2}{2m_c} + E_g - \omega_0, \\ \epsilon_{vk} &= -\frac{k^2}{2m_v}. \end{aligned} \tag{5.3}$$

In the next step, the reduced density matrix, which has been calculated from the Bloch equations, is used to evaluate the potential propagator.

VI. NUMERICAL RESULTS

We calculate the two-time-dependent retarded screened Coulomb potential by using the carrier distributions determined from the numerical solutions of the semiconductor Bloch equations, Eq. (5.1). With these carrier distributions we will solve the integral equation (4.4) directly and compare the solution with the time-dependent plasmon pole approximation.

For illustrative purpose, we use for the investigation of $V^r(t_1, t_2)$ relatively long pulses, so that the plasma frequency does not change too much during one oscillation period. The changes of w_{pl} can be seen in S_q. We solve the Bloch equations (5.1) for a Gaussian laser pulse envelope

$$dE(t) = Ae^{-t^2/\tau^2}. \tag{6.1}$$

For the pulse width τ we take 200 fs, the detuning is $\delta = \omega_0 - E_g = 3E_0$, and the amplitude corresponds to a π pulse

$$\int_{-\infty}^{\infty} dt\, 2dE(t) = \pi. \tag{6.2}$$

This definition of a π pulse is valid only if the internal field contribution, i.e., the term $\sum VP$ in Eq. (5.2), is neglected. In general the internal field can be of the same order[23] and gives rise to an increased effective field. However, this local field, which leads to the formation of excitons, acts not directly as a driving field, because it is complex.

The time-dependent plasma frequency defined in Eq. (4.2) is shown in Fig. 2. GaAs parameters are used throughout: $E_0 = 4.2$ meV, $a_0 = 14$ nm, $m_c/\mu = 1.284$, and $m_v/\mu = 4.522$, where μ is the reduced electron-hole mass.

Together with the initial value $S_q(t_2, t_2) = 0$, Eq. (4.4) defines a recursive scheme in t_1 for every given t_2. The results for $t_2 = -150$ fs are shown in Fig. 3. Figure 3(b) shows S_q for $qa_0 = 0, 0.6$, and 1.2. A comparison with Fig. 2 reveals that the frequency of the oscillation is indeed given by the plasma frequency at time t_1, in agreement with Eq. (4.5). Similar results have been obtained by Hartmann, Stolz, and Zimmerman[17] using equilibrium carrier distributions with a time-dependent temperature and chemical potential. A similar statement holds for $q \neq 0$, but then the frequency is given by the plasmon dispersion ω_q at time t_1 for the nonequilibrium distribution.[7] For $qa_0 < 1$ the plasmon mode suffers no Landau damping. At higher momenta it enters the pair continuum and gets damped out quickly.

One usually defines the Fourier transform of the screened potential by

$$V_q(\omega, T) = \int_0^{\infty} d\tau e^{i\omega\tau} V_q^r(T + \tau/2, T - \tau/2), \tag{6.3}$$

where $T = (t_1 + t_2)/2$ is the center and $\tau = t_1 - t_2$ is the relative time.[17] This representation is useful for weakly time-dependent distributions. If the distributions are constant, $V_q(\omega, T)$ is nothing but the well-known dynamically screened Coulomb potential defined by the Lindhard formula.[9,21] The time integral in Eq. (6.3) runs over the past *and* the future. In equilibrium theory this is no problem, but in nonequilibrium situations the future is unknown. Thus the definition (6.3) cannot be used in quantum kinetics. We propose instead

$$V_q(\omega, t_1) = \int_{-\infty}^{t_1} dt_3 e^{i\omega(t_1 - t_3)} V_q^r(t_1, t_3) = \int_0^{\infty} d\tau e^{i\omega\tau} V_q^r(t_1, t_1 - \tau) \tag{6.4}$$

and correspondingly

$$\epsilon_q^{-1}(\omega, t_1) = 1 + \int_{-\infty}^{t_1} dt_3 e^{i(\omega + i2\gamma)(t_1 - t_3)} S_q(t_1, t_3). \tag{6.5}$$

The quantity defined in (6.4) also approaches in the limit $t_1 \to \infty$ the Lindhard result, but it reflects the correct causal structure, because only the past is involved.

The time-dependent inverse dielectric function is evaluated for a $\pi/2$-laser pulse with a width of $\tau = 50$ fs and zero detuning. The pulse envelope together with the time-dependent plasma frequency is shown in Fig. 4. The time-dependent inverse dielectric function is shown in Fig. 5 for $qa_0 = 1$ and $\gamma = 0$. Up to $t_1 \simeq 90$ fs the ϵ^{-1}

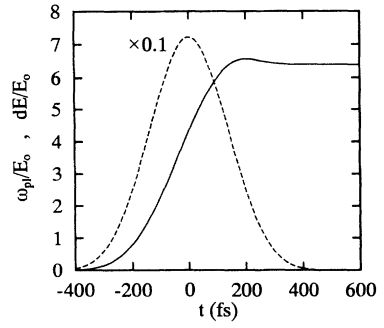

FIG. 2. Plasma frequency $\omega_{\rm pl}(t)$ (solid line) after an excitation with a π-laser pulse (pulse width $\tau = 200$ fs, detuning $3E_0$) and envelope function $dE(t)$ of the pulse (dashed line).

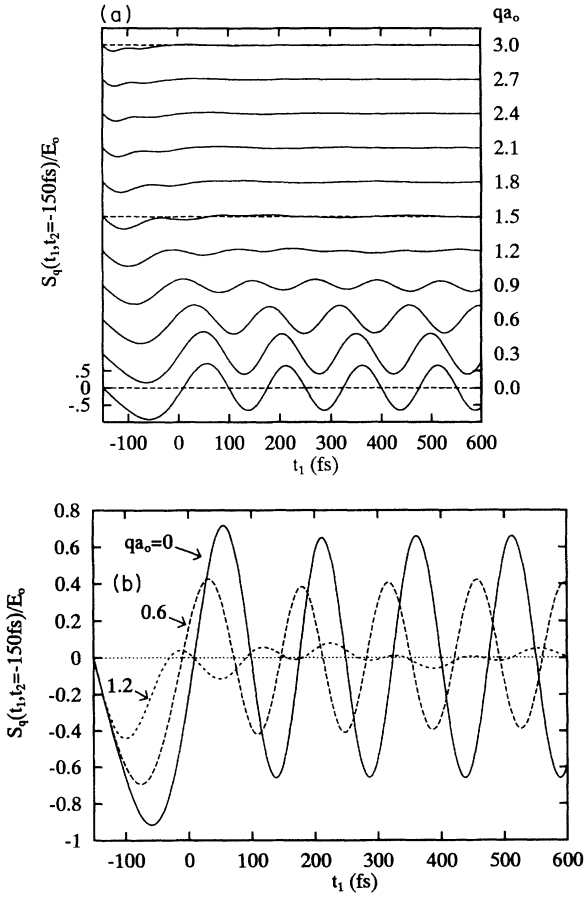

FIG. 3. Density correlation function $S_q(t_1, t_2 = -150$ fs) for the pulse of Fig. 2 versus time t_1. (a) for various momenta $0 \leq qa_0 \leq 3$. (b) for $qa_0 = 0, 0.6$, and 1.2.

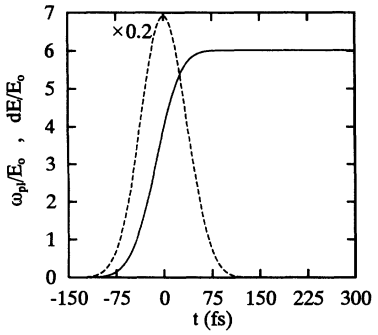

FIG. 4. Plasma frequency $\omega_{\rm pl}(t)$ (solid line) after an excitation with a $\pi/2$-laser pulse (pulse width $\tau = 50$ fs, zero detuning) and envelope function $dE(t)$ of the pulse (dashed line).

is very flat. At only one plasma oscillation period after the pulse, $t_1 \simeq 160$ fs, does a broadened plasmon-pole-like structure emerges. The finite time interval causes the small oscillation seen in Fig. 5. If a finite γ is used, these oscillations are damped.

To gain further insight, we compare $\epsilon^{-1}(\omega, t_1)$ with the time-dependent plasmon-pole model of Eq. (4.18). The laser-pulse duration is small compared to the plasma oscillation period. Therefore we can take

$$\omega_{\rm pl}(t_1) \approx \Theta(t_1 - t_0)\omega_{\rm pl}^{\max}, \tag{6.6}$$

where t_0 is the time of the pulse maximum, i.e., zero. This results in

$$\epsilon_q^{-1\rm PP}(\omega, t_1) = 1 + \int_0^{t_1} d\tau e^{i\omega\tau} S_q^{\rm PP}(\tau),$$
$$S_q^{\rm PP}(\tau) = -\frac{\left(\omega_{\rm pl}^{\max}\right)^2}{\omega_q} \sin(\omega_q\tau) e^{-\Gamma\tau}. \tag{6.7}$$

The time integration runs only over the finite interval $[0, t_1]$. This leads to a broadening of the inverse dielectric function of the order $1/t_1$ (uncertainty relation).

In Fig. 6 the ϵ^{-1} and $\epsilon^{-1\rm PP}$ are shown. The parameters

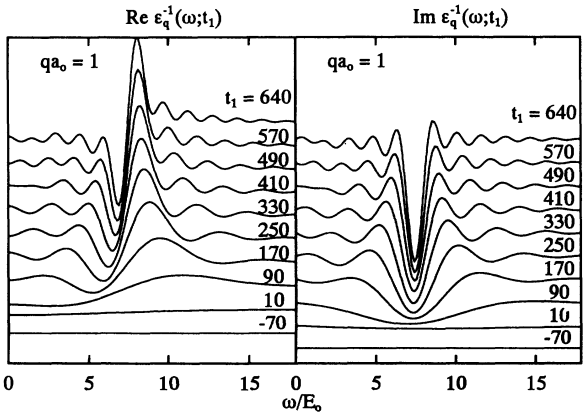

FIG. 5. Real part (left) and imaginary part (right) of the calculated inverse time-dependent dielectric function $\epsilon_q^{-1}(\omega, t_1)$ for the pulse of Fig. 4 versus frequency ω/E_0 for various times t_1 and a momentum $qa_0 = 1$.

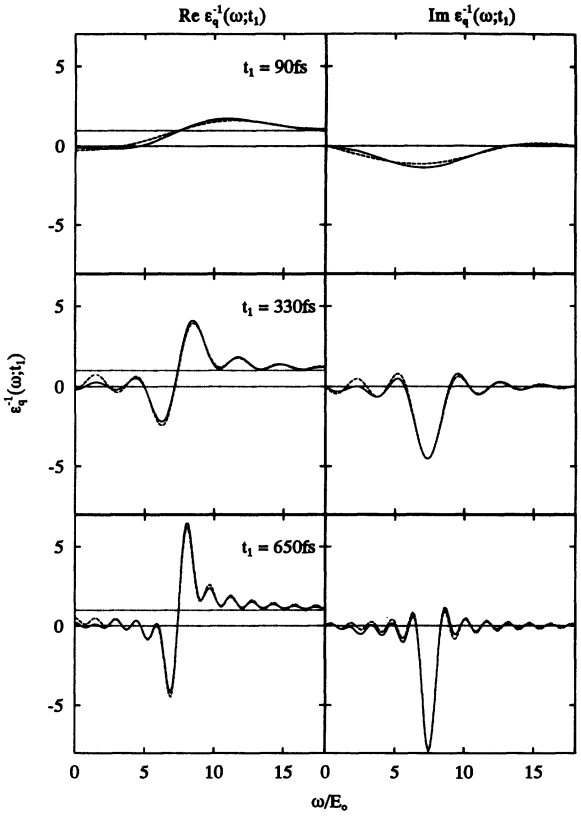

FIG. 6. Real part (left row) and imaginary part (right row) of the calculated inverse time-dependent dielectric function $\epsilon_q^{-1}(\omega, t_1)$ (solid line) as in Fig. 4 and a plasmon-pole approximation (dashed line) versus frequency ω/E_0 for $t_1 = 90$ fs, 330 fs, and 650 fs and a momentum $qa_0 = 1$.

used in Fig. 6 are listed in Table I.

For ω_q we used a slightly larger value than the plasma frequency in order to model the dispersion. The small time-drift in the values of ω_q reflects that the average frequency still has a small time-dependence. At $qa_0 = 1$ the mode still suffers no Landau damping. But we used a nonzero damping Γ in order to model the influence of the initial amplitude variation, due to the initially increasing plasma frequency. The figure shows that the time-dependent plasmon-pole approximation gives an excellent description of the femtosecond dynamic of screening.

VII. CONCLUSION AND DISCUSSION

We calculated the retarded Coulomb Keldysh-propagator in the time domain for a time-dependent car-

TABLE I. Parameters used in Fig. 6.

t_1 (fs)	$\omega_q(E_0)$	$\Gamma(E_0)$
90	6.70	0.80
330	7.39	0.18
650	7.45	0.15

rier distribution, which we get from the solution of the full semiconductor Bloch equations of the coherent evolution of the system driven by a short laser pulse. We found that the two-time potential propagator oscillates with the plasmon dispersion, determined by the carrier distribution at the latest time.

With a proper definition of a frequency-dependent retarded potential we showed that in the ultra-short-time domain the plasmon resonance of screened potential broadens with an effective width given by the uncertainty relation $\Delta\omega \lesssim \Delta t^{-1}$. For an initial time period of $\Delta t \leq \omega_{\mathrm{pl}}^{-1}$, i.e., when the broadening is larger or comparable to the plasma frequency, there is essentially no screening. A two-time-dependent plasmon-pole approximation is derived and shown to give an excellent description of the femtosecond dynamics of screening.

ACKNOWLEDGMENTS

We appreciate interesting discussions with our colleagues L. Bányai and C. Ell. This work has been supported by the Deutsche Forschungsgemeinschaft and the Volkswagen Stiftung.

[1] J.Y. Bigot, M.T. Portella, R.W. Schoenlein, J.E. Cunningham, and C.V. Shank, Phys. Rev. Lett. **67**, 636 (1991).
[2] T. Elsaesser, J. Shah, L. Rota, and P. Lugli, Phys. Rev. Lett. **66**, 1757 (1991).
[3] M. Wegener, D.S. Chemla, S. Schmitt-Rink, and W. Schäfer, Phys. Rev. A **42**, 5675 (1990).
[4] P.C. Becker, H.L. Fragnito, C.H. Brito Cruz, R.L. Fork, J.E. Cunningham, J.E. Henry, and C.V. Shank, Phys. Rev. Lett. **61**, 1647 (1988).
[5] J.L. Oudar, D. Hulin, A. Mingus, A. Antonetti, and F. Alexandre, Phys. Rev. Lett. **55**, 2074 (1985).
[6] D.C. Scott, R. Binder, and S.W. Koch, Phys. Rev. Lett. **69**, 347 (1992).
[7] K. El Sayed, R. Binder, D.C. Scott, and S.W. Koch, Phys. Rev. B **47**, 10 210 (1993).
[8] K. El Sayed and H. Haug, Phys. Status Solidi B **173**, 189 (1992).
[9] H. Haug and S.W. Koch, *Quantum Theory of the Optical and Electronic Properties of Semiconductors*, 2nd ed. (World Scientific, Singapore, 1993).
[10] H. Haug and C. Ell, Phys. Rev. B **46**, 2126 (1992).
[11] A.V. Kuznetsov, Phys. Rev. B **44**, 8721 (1991).
[12] D.B. Tran Thoai and H. Haug, Z. Phys. B **91**, 199 (1993).
[13] P. Lipavský, V. Špička, and B. Velický, Phys. Rev. B **34**, 6933 (1986); P. Lipavský, F. S. Kahn, A. Kalvová , and J.W. Wilkins, *ibid.* **43**, 6650 (1991).
[14] A.P. Jauho, in *Granular Nanoelectronics*, edited by D.K. Ferry (Plenum, New York, 1991), p. 133.
[15] D.F. DuBois, in *Lectures in Theoretical Physics IX C, Kinetic Theory*, edited by W.E. Britten, A.O. Barut, and M. Guenin (Gordon and Breach, New York, 1967), p. 469.
[16] L.D. Landau and E.M. Lifshitz, *Course of Theoretical Physics Vol. X, Physical Kinetics* (Pergamon, Oxford, 1981).
[17] M. Hartmann, H. Stolz, and R. Zimmermann, Phys. Status Solidi B **159**, 35 (1990).
[18] L.P. Kadanoff and G. Baym, *Quantum Statistical Mechanics* (W.A. Benjamin, New York, 1962).
[19] K. Henneberger and H. Haug, Phys. Rev. B **38**, 9759 (1988).
[20] H. Haug, Phys. Status Solidi B **173**, 139 (1992).
[21] G.D. Mahan, *Many-Particle Physics* (Plenum, New York, 1986).
[22] H. Haug and S. Schmitt-Rink, Prog. Quantum Electron. **9**, 3 1984.
[23] R. Binder, S.W. Koch, M. Lindberg, and N. Peyghambarian, Phys. Rev. Lett. **65**, 899 (1990).